ISBN: 978-981-18-3959-7
2022 the 12th International Workshop on Computer Science and Engineering (WCSE 2022)
doi: 10.18178/wcse.2022.06.036

Multi-target Localization Technology Fused with Clustering Algorithm

Chen Cheng [1], Li Ning [1+], Guo Yan[1], Sheng Jinfeng and Li Huajing[1]

[1] School of Communication Engineering, Army Engineering University of PLA

Abstract. At present, wireless sensor networks are widely used in passive target localization. Aiming at the problem of low positioning accuracy in the compressed sensing localization algorithm based on Bayesian learning, a multi-target localization technology fused with clustering algorithm is proposed. Firstly, the multi-target problem is transformed into sparse signal reconstruction problem by Using Bayesian learning algorithm. Then, based on the target location obtained by multiple sparse recovery, clustering operation is performed to achieve accurate location. Simulation results show that the proposed method improves positioning accuracy and has strong robustness.

Keywords: Wireless sensor network ; Bayesian learning ; Compression perception ; Clustering algorithm ; Sparse signal reconstruction

1. Introduction

In recent years, with the increasing demand for location based services (LBS), precise positioning technology has received more and more urgent attention[1]. At present, the most widely used positioning technology is the Global Navigation Satellite System (GNSS), which implements the positioning function according to the wireless signal sent by the navigation satellite [2].In the case of occlusion and non-line of sight distance, the positioning performance will be greatly affected [3]. In order to solve the problem of limited positioning of GNSS under obstruction, wireless sensor networks (Wireless Sensor Networks, WSN) have been applied to DFL, and are gradually used in indoor positioning, wildlife tracking, intruder monitoring, and survivor search and rescue scenarios. Development [4].

Passive and passive target positioning based on wireless signals can be based on the time of arrival (Time Of Arrival, TOA) [5], Time Difference Of Arrival (TDOA) [6], Angle Of Arrival (AOA) [7], Received Signal Strength (RSS) [8] and other signal indicators to obtain measurement data, and estimate the target position by analyzing the influence of wireless signals.

At present, DFL technologies based on WSN can be classified into four categories: (1) Passive target location technology based on geometric structure [9]; (2) Passive target location technology based on fingerprint [10]; (3) Wireless layer based Passive target location technology based on radio Tomographic Imaging (RTI) [11]; (4) Passive target location technology based on Compressive Sensing (CS) [12]. CS technology provides a new idea for realizing DFL. In CS-based DFL, only a small amount of measurement data can be collected to reconstruct the target position vector with high probability.

One of the keys to the construction of the observation matrix in CS is that the observation matrix and the sparse representation matrix satisfy the restricted equidistant characteristic (RIP) characteristics. The stronger the RIP attribute, the higher the reconstruction accuracy.

The sparse reconstruction algorithm in CS is the core of CS theory and the key to reconstruct the original signal. There are currently three representative sparse reconstruction algorithms: Basic Pursuit (BP) algorithm [13], Orthogonal matching pursuit (OMP) algorithm [14] and Sparse Bayesian Learning (SBL) algorithm [15]. The SBL algorithm can not only reconstruct the sparse signal, but also realize the estimation of the noise, increase the credibility of the signal, and the algorithm can still maintain good reconstruction performance when the RIP is weak. Among them, the sparse reconstruction algorithm based on Variational

+ Corresponding author. Tel.: +86-13357834568
E-mail address:js_ningli@sina.com.

Bayesian Inference (VBI) shows a good reconstruction effect. Therefore, this technology uses a VBI-based sparse reconstruction algorithm for CS reconstruction.

However, although the CS multi-target positioning technology based on the VBI sparse reconstruction algorithm [16] can realize the positioning function, However, although the CS multi-target positioning technology based on the VBI sparse reconstruction algorithm can realize the positioning function, it still cannot achieve precise positioning.

In response to the above problems, this paper proposes a multi-target positioning technology based on the clustering algorithm. The main contributions of this article are:

(1) The clustering algorithm has good compatibility with the target location optimization problem. The effective combination of the clustering algorithm realizes the accurate estimation of the target position without increasing the complexity of the algorithm.

(2) This algorithm can effectively resist noise and enhance positioning stability.

2. Compressed Sensing Theory

2.1. Basic Problem Description

If a signal contains at most K non-zero elements, and K is much smaller than N($N \ll K$) ,it is a K-order sparse signal. According to the definition, the set of K-order sparse signals can be expressed as:

$$\mathbb{S}_K = \left\{ \theta : \|\theta\|_0 \le K \right\} \tag{1}$$

For the sparse signal θ, the observation matrix $\Phi \in \mathbb{R}^{M \times N}$ is under-sampled at a rate lower than the Nyquist sampling rate to obtain the observation vector $\mathrm{y} \in \mathbb{R}^{M \times 1}$. According to the theory of compressed sensing, the original signal θ can be reconstructed with high probability according to the observation vector y. Specifically, the observation vector can be expressed as the following form:

$$\mathrm{y} = \Phi\theta + \varepsilon \tag{2}$$

where $\varepsilon \in \mathbb{R}^{M \times 1}$ is the measurement noise vector. Figure 1 shows the sparse signal perception model. Among them, the M-dimensional observation vector y can be represented by the observation matrix Φ and the sparse signal θ.

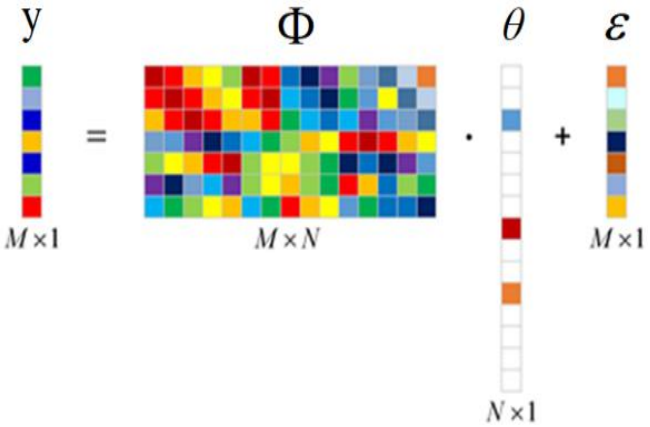

Fig. 1: Sparse Signal Perception Model

2.2. Sparse Reconstruction Algorithm

The sparse reconstruction algorithm is the key to reconstruct the original signal. It is that the observation value y obtained by the observation matrix Φ is under-sampled data. Using the compressed sensing sparse reconstruction algorithm, the most sparse signal can be solved as the reconstructed signal θ when the measurement noise ε, the observation matrix Φ, and the observation vector y are known. The specific expression is:

$$\min_s \|\theta\|_0, \text{ s.t. } \mathrm{y} = \Phi\theta + \varepsilon \tag{3}$$

In order to measure the sparsity of signal θ, the number of non-zero elements in the signal, the ℓ_0 norm of θ is used as the sparsity index.

The measurement model of the sparse vector reconstruction algorithm based on variational Bayesian inference is as follows:

$$\mathrm{y}=\Psi^{(1)}\omega^{(1)}+\Psi^{(2)}\omega^{(2)}+\varepsilon \tag{4}$$

where $\Psi^{(1)}\in\mathbb{R}^{\mathrm{M}\times\mathrm{N}}$ and $\Psi^{(2)}\in\mathbb{R}^{\mathrm{M}\times\mathrm{N}}$ are known matrices; $\varepsilon\in\mathbb{R}^{N\times1}$ are measurement noise vectors; $\omega^{(1)}\in\mathbb{R}^{\mathrm{N}\times1}$ and $\omega^{(2)}\in\mathbb{R}^{\mathrm{N}\times1}$ are sparse representation coefficients. According to the dictionary environment parameter values, vectors $\omega^{(1)}$ and $\omega^{(2)}$ have a common support set $\mathbb{T}\subseteq\{1,2,...,N\}$. In this sparse representation model, in order to estimate the target position vector θ, $\omega^{(1)}$ and $\omega^{(2)}$ need to be reconstructed at the same time to obtain the common support set of the two to realize joint sparse reconstruction. In order to induce the joint sparsity of $\omega^{(1)}$ and $\omega^{(2)}$, we established a two-layer Gaussian prior model. The two-level prior distribution can be expressed as:

$$p(\omega^{(1)};a,\boldsymbol{b})=\int p(\omega^{(1)}\mid\boldsymbol{\alpha})p(\boldsymbol{\alpha};a,\boldsymbol{b})\mathrm{d}\boldsymbol{\alpha} \tag{5}$$

$$p(\omega^{(2)};a,\boldsymbol{b})=\int p(\omega^{(2)}\mid\boldsymbol{\alpha})p(\boldsymbol{\alpha};a,\boldsymbol{b})\mathrm{d}\boldsymbol{\alpha} \tag{6}$$

where α_n^{-1} represents the variance of the $\omega^{(1)}$ and nth component $w_n^{(1)}$, And define $\boldsymbol{\alpha}=[\alpha_1,\alpha_2,...,\alpha_N]^T$. $w_n^{(2)}=\Omega\cdot w_n^{(1)}$, The variance of $w_n^{(2)}$ is $\Omega^2\cdot\alpha_n^{-1}$, and Ω represents the ratio of the minimum signal attenuation to the maximum signal attenuation on the link.

$$p(\omega^{(1)}\mid\boldsymbol{\alpha})=(2\pi)^{-\frac{N}{2}}\left|\Lambda\right|^{\frac{1}{2}}\exp(-\frac{1}{2}(\omega^{(1)})^T\Lambda\omega^{(1)} \tag{7}$$

$$p(\omega^{(2)}\mid\boldsymbol{\alpha})=(2\pi)^{-\frac{N}{2}}\left|\Lambda\right|^{\frac{1}{2}}\exp(-\frac{1}{2}(\omega^{(2)})^T\Lambda\omega^{(2)} \tag{8}$$

where $\Lambda=diag(\boldsymbol{\alpha})$.

$$p(\boldsymbol{\alpha};a,\boldsymbol{b})=\prod_{n=1}^{N}\frac{1}{\Gamma(a)}d_n^a\alpha_n^{a-1}.\exp(-b_n\alpha_n) \tag{9}$$

where a and b_n are the parameters of the α_n prior distribution, and $\boldsymbol{b}=[b_1,\ldots,b_N]^T$. $\Gamma(a)=\int_0^\infty x^{a-1}e^{-x}\mathrm{d}x$ represents the gamma function.

Using variational Bayesian inference to estimate the posterior distribution of hidden variables, it can be expressed as:

$$q^*(\mathbf{w}^{(1)})=\mathcal{N}(\mathbf{w}^{(1)}\mid\boldsymbol{\mu}^{(1)},\boldsymbol{\Sigma}^{(1)}) \tag{10}$$

$$\text{where }\boldsymbol{\mu}^{(1)}=\langle\beta\rangle_{q(\beta)}\boldsymbol{\Sigma}^{(1)}(\boldsymbol{\Psi}^{(1)})^T(\mathbf{y}-\boldsymbol{\Psi}^{(2)}\boldsymbol{\mu}^{(2)}) \tag{11}$$

$$\boldsymbol{\Sigma}^{(1)}=\langle\beta\rangle_{q(\beta)}(\boldsymbol{\Psi}^{(1)})^T\boldsymbol{\Psi}^{(1)}+\langle\boldsymbol{\Lambda}\rangle_{q(\boldsymbol{\alpha})}^{-1} \tag{12}$$

$\boldsymbol{\mu}^{(1)}$ is the mean vector of the posterior distribution of $\mathbf{w}^{(1)}$, and $\boldsymbol{\Sigma}^{(1)}$ is the covariance matrix of the posterior distribution of $\mathbf{w}^{(1)}$.

$$q^*(\mathbf{w}^{(2)})=\mathcal{N}(\mathbf{w}^{(2)}\mid\boldsymbol{\mu}^{(2)},\boldsymbol{\Sigma}^{(2)}) \tag{13}$$

$$\text{where }\boldsymbol{\mu}^{(2)}=\langle\beta\rangle_{q(\beta)}\boldsymbol{\Sigma}^{(2)}(\boldsymbol{\Psi}^{(2)})^T(\mathbf{y}-\boldsymbol{\Psi}^{(1)}\boldsymbol{\mu}^{(1)}) \tag{14}$$

$$\boldsymbol{\Sigma}^{(2)}=\langle\beta\rangle_{q(\beta)}(\boldsymbol{\Psi}^{(2)})^T\boldsymbol{\Psi}^{(2)}+\langle\boldsymbol{\Lambda}\rangle_{q(\boldsymbol{\alpha})}^{-1} \tag{15}$$

where $\boldsymbol{\mu}^{(2)}$ is the mean vector of the posterior distribution of $\mathbf{w}^{(2)}$, and $\boldsymbol{\Sigma}^{(2)}$ is the covariance matrix of the posterior distribution of $\mathbf{w}^{(2)}$.

$$q^*(\beta)=\text{Gamma}(\beta \mid \tilde{c}, \tilde{d}) \tag{16}$$

where

$$\tilde{c}=c+\frac{M}{2} \tag{17}$$

$$\left\|\mathbf{y}-\boldsymbol{\Psi}^{(1)}\boldsymbol{\mu}^{(1)}-\boldsymbol{\Psi}^{(2)}\boldsymbol{\mu}^{(2)}\right\|_2^2+\text{tr}\ \boldsymbol{\Psi}^{(1)}\boldsymbol{\Sigma}^{(1)}(\boldsymbol{\Psi}^{(1)})^T+\text{tr}\ \boldsymbol{\Psi}^{(2)}\boldsymbol{\Sigma}^{(2)}(\boldsymbol{\Psi}^{(2)})^T \tag{18}$$

$\tilde{c}$ and $\tilde{d}$ are the deterministic parameters of the posterior distribution of β, which can be expressed as：

$$\langle\beta\rangle_{q(\beta)}=\frac{\tilde{c}}{\tilde{d}} \tag{19}$$

$$q^*(\boldsymbol{\alpha})=\prod_{n=1}^{N}\text{Gamma}(\alpha_n \mid \tilde{a}, \tilde{b}_n) \tag{20}$$

where

$$\tilde{a}=a+1 \tag{21}$$

$$\tilde{b}_n=b_n+\frac{1}{2}\,\mu_n^{1\,2}+\frac{1}{2}\Sigma_{n,n}^1+\frac{1}{2}\,\mu_n^{2\,2}+\frac{1}{2}\Sigma_{n,n}^2 \tag{22}$$

$\tilde{a}$ and $\tilde{b}_n$ are the deterministic parameters of the posterior distribution of $\boldsymbol{\alpha}$, and $\tilde{\boldsymbol{b}}=[\tilde{b}_1,\ldots,\tilde{b}_N]^T$. $\mu_n^{(1)}$ and $\mu_n^{(2)}$ represent the nth component of $\boldsymbol{\mu}^{(1)}$ and $\boldsymbol{\mu}^{(2)}$, respectively. $\Sigma_{n,n}^{(1)}$ and $\Sigma_{n,n}^{(2)}$ represent the nth main diagonal element of $\boldsymbol{\Sigma}^{(1)}$ and $\boldsymbol{\Sigma}^{(2)}$, respectively.

Based on the above results, the sparse vector can be reconstructed by iteratively updating the hidden variables $\mathbf{w}^{(1)}$, $\mathbf{w}^{(2)}$ and the posterior distributions of β and $\boldsymbol{\alpha}$.

3. Clustering Algorithm

Clustering algorithm is a method of statistical classification of research objects. According to the similarity of research objects, objects with similar characteristics are classified into the same category (cluster). This paper uses the K-means clustering algorithm in the clustering algorithm. Specific steps are as follows:

Step 1: The initial cluster center point. Select K data points from the data points as the initial cluster center points.

Step 2: According to the Euclidean distance to K cluster center points, the data points are assigned to the cluster center point with the shortest Euclidean distance to form K clusters.

Step 3: Update the cluster center point. Calculate the arithmetic average of the data points in each cluster, and use the arithmetic average point as the new cluster center point to update the cluster center point, and calculate the distance and the distance from all points to the respective cluster center point after the clustering is completed. .

Step 4: Iteratively update and stop. Compare whether the sum of the distances from all points to the respective cluster center points after two clusters before and after the cluster is equal, if they are not equal, update the cluster and the cluster center points circularly, if they are the same, end the loop.

Step 5: The output result is the position of the cluster center point.

4. Multi-target Positioning Technology Fused with Clustering Algorithm

4.1. Positioning Model

The multi-target localization model fused with Clustering Algorithm (CA) is shown in Figure 2. First, grid the ground monitoring area. Divide the monitoring area into N square grids of the same size, namely 1,2,3，…,n, …,N. The N-dimensional vector $\theta_{N\times1}$ is used to characterize the K target position information. Because K is much smaller than N, $\theta_{N\times1}$ is a sparse vector. If there is a target in the nth grid in the grid, the

nth component of the sparse vector $\theta_{N\times1}$ is set to 1, that is, θ_n=1, and the rest are 0. And the center point of the grid is specified as the estimated target position.

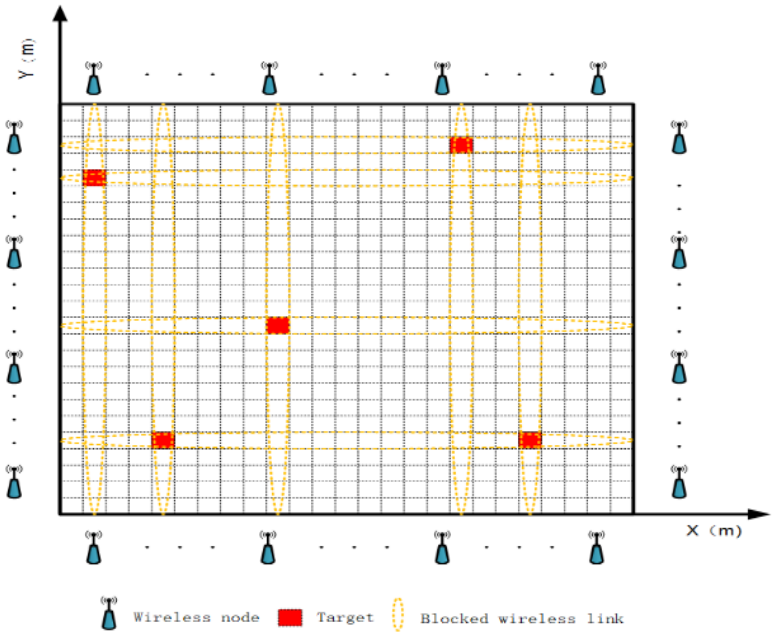

Fig. 2: Passive target localization model fused with clustering algorithm

The sensors deployed around the monitoring area are used to collect the RSS changes of M wireless links in the monitoring area to reflect the shadow effect caused by the target and estimate the target position. K targets are randomly placed in the monitoring area, and the RSS change value on the m-th wireless link is measured. According to the formula, the received signal strength variation ΔR_m^t of the m-th link at any time t can be expressed as:

$$\Delta R_m^t = \Delta C_m + \Delta v_m \tag{23}$$

where ΔC_m represents the amount of signal attenuation in time t, and Δv_m represents the change in the measured noise during the time t. It can be seen from the above that the received signal strength is only related to the target position and the change in measurement noise. Since there is no target in the monitoring area at the initial time t_0, there are:

$$\Delta C_m = C_m^t \tag{24}$$

where C_m^t represents the received signal strength value on the m-th link at time t.

Because the signal received by the wireless sensor is affected by multiple targets at the same time, when there are multiple targets in the monitoring area, and each target satisfies the sparse distribution, it can be considered as a linear superposition of the shadow effect caused by multiple targets on the m-th link , Then the change of received signal strength on the m-th wireless link is calculated by the formula as:

$$C_m^t = \sum_{n=1}^{N} \theta_n \phi_{m,n} \tag{25}$$

where θ_n represents the nth element of the target position vector $\theta \in \mathbb{R}^{N\times1}$. $\phi_{m,n}$ is the sparse representation of the (m,n) element of dictionary $\Phi \in \mathbb{R}^{M\times N}$. According to the formula, the received signal strength change on M links can be expressed as:

$$y = \Phi\theta + \varepsilon \tag{26}$$

where $y \in \mathbb{R}^{M\times1}$ is the observation vector, and its m-th element is $y_m = \Delta R_m^t$; $\varepsilon \in \mathbb{R}^{M\times1}$ is the noise vector, and its m-th element is $\varepsilon_m = \Delta v_m$; θ is a K-order sparse vector.

4.2. Saddle Model Dictionary

The schematic diagram of the target influence area of the saddle model is shown in Figure 3.

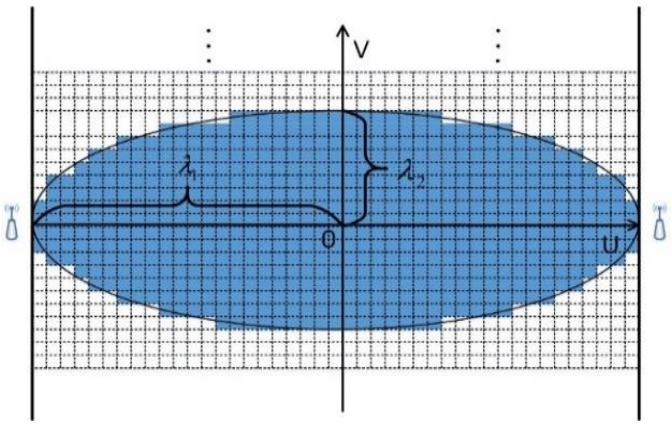

Fig. 3: Schematic diagram of the affected area of the saddle model

The affected area of the saddle model is elliptical. The semi-major axis of the ellipse is λ_1, the semi-minor axis is λ_2, and the midpoint of the link is the origin, and the line of sight of the link is the horizontal axis to establish a $U-V$ coordinate system. The grid satisfies the conditions:

$$\frac{U_{m,n}^2}{\lambda_1^2}+\frac{V_{m,n}^2}{\lambda_2^2}\le 1 \tag{27}$$

where $(U_{m,n},V_{m,n})$ represents the coordinate of the grid n relative to the link m, and the dark color represents the grid that meets the constraint conditions. For a grid in an elliptical area, if there is a target in the grid, its influence on the received signal strength on link m can be expressed as:

$$\phi_{m,n}=\gamma\left(\frac{1-\Omega_m}{\lambda_1^2}U_{m,n}^2+\Omega_m\left(1-\frac{V_{m,n}^2}{\lambda_2^2}\right)\right) \tag{28}$$

where γ is the maximum attenuation of the received signal strength, and Ω_m is the ratio of the minimum signal attenuation on the link to γ.

4.3. Mesh Pruning Mechanism in Sparse Restoration

Due to the influence of noise, the reconstructed sparse vector $\hat{\theta}$ will be less strictly sparse. Noise interference can be eliminated by threshold setting η_{th}, and get the ideal reconstructed sparse vector $\hat{\theta}$ and target position p_1. The estimation formula of the support set $\hat{\Omega}$ of the target position vector is as follows:

$$\hat{\Omega}=\left\{n\left|20\lg\left(\frac{[\hat{\boldsymbol{\theta}}]_n}{\max\limits_i[\hat{\boldsymbol{\theta}}]_i}\right)\ge\eta_{th}\right.\right\} \tag{29}$$

After trimming, the support set of the target position can be obtained, and the target position can be estimated. The coordinate set is as follows:

$$\left\{(x_n,y_n)\middle|n\in\hat{\Omega}\right\} \tag{30}$$

Compressed sensing positioning technology to obtain 10 sets of target positions, namely $p_1\ldots p_{10}$, and renumber these coordinates as: $p=(x_1,x_2,...x_i,...,x_{10K};y_1,y_2,...y_i,...,y_{10K})$ Use these 10 sets of data as the initial clustering points of the clustering algorithm for clustering operations. First initialize the data and set the initial clustering center point. In order to reduce the number of iterations, the initial clustering center point we set should not be too concentrated, so we use the first estimated K target estimated points as the initial clustering center point. Then the data points are clustered according to the Euclidean distance between each point and the K cluster center points. The Euclidean distance formula is as follows:

$$d_{ik}=\sqrt{(x_i-\overline{x_k})^2+(y_i-\overline{y_k})^2} \tag{31}$$

where (x_i, y_i) represents the coordinates of the i-th data point, $i = 1,2,...,10K$; $(\overline{x_k}, \overline{y_k})$ represents the coordinates of the k-th cluster center point, $k = 1,2,...,K$; d_{ik} represents the Euclidean distance from the i-th data point to the k-th cluster center point. The corresponding data points in the clusters are expressed as: $c_k = (x_{k1}, x_{k2}, ...; y_{k1}, y_{k2}, ...)$ .The number of data points in the cluster is variable. After the classification is completed, the sum of the distances D from all points to the respective cluster centers is calculated:

$$D = \sum_{i=1}^{K} d_{i\min} \tag{32}$$

The way to update cluster center point $(\overline{x_k}, \overline{y_k})$ is to take the arithmetic average of the data points in each cluster. Because the number of data points in the cluster is uncertain, we assume it is m, then:

$$\overline{x_k} = \frac{1}{m} \sum_{i=1}^{m} x_{ki} \tag{33}$$

$$\overline{y_k} = \frac{1}{m} \sum_{i=1}^{m} y_{ki} \tag{34}$$

Update the coordinates of the data points and the cluster center in the cluster, and loop iteratively until the iterative conditions are met, and then jump out of the loop.

Finally, output the result: record the coordinates of the last cluster center point and use it as the final estimated target position $p = (\overline{x_1}, \overline{x_2}, ..., \overline{x_K}; \overline{y_1}, \overline{y_2}, ..., \overline{y_K})$.

5. Experimental Simulation and Result Analysis

This section verifies the performance of the proposed positioning algorithm through simulation. Among them, the target monitoring area is a 14m×14m square area, which is divided into N=784 square grids of the same size, and the number of links covering this area is M=56.Assume $\Delta\varepsilon_m(f)$ is additive white Gaussian noise, and define the signal-to-noise ratio. $SNR(dB) \triangleq 10\lg(\left\|\Phi\omega^f\right\|_2^2 / M\sigma^2)$. In order to evaluate the positioning performance of this algorithm, the average positioning error (ALE) and accuracy are respectively defined as the evaluation indicators. ALE is the average Euclidean distance between the estimated target position value and the true position value; the accuracy rate is the percentage of correct estimation between the estimated target position value and the true position value. The results are as follows:

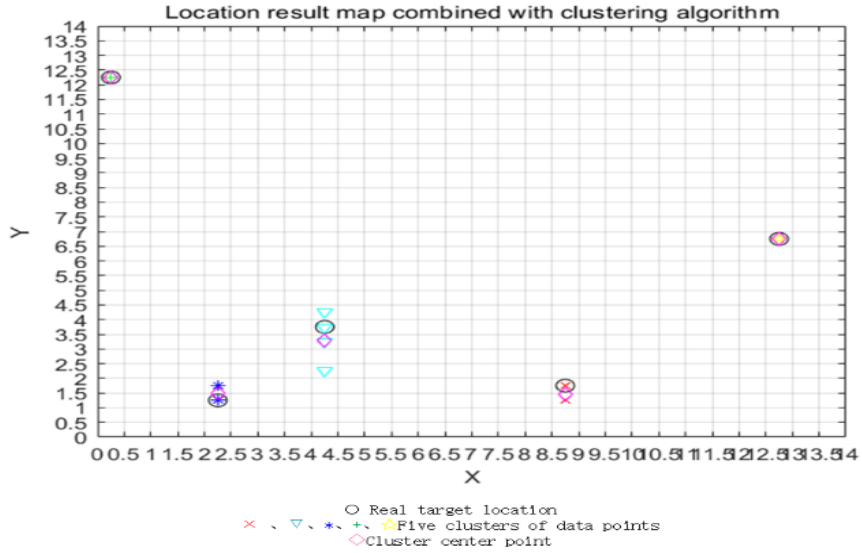

Fig.4: The localization result map of the fusion clustering operation

By comparing the estimated target position of the final clustering center point with the actual target position, it can be seen that the multi-target positioning technology fused with the clustering algorithm accurately estimates the true target position and realizes the precise positioning of multiple targets.

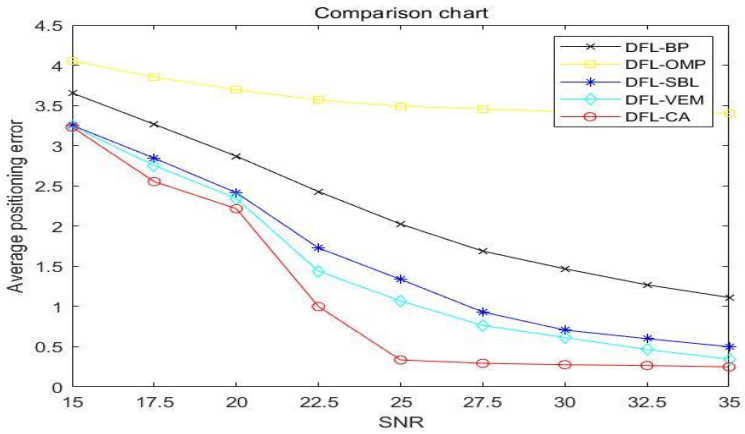

Fig.5 Comparison of positioning errors of several positioning algorithms

Figure 5 shows a comparison chart of the average positioning errors of various algorithms under different conditions of sex-to-noise ratios obtained after multiple experiments. It can be seen that this method has obvious advantages compared with other types of methods. Longitudinal comparison shows that in the 15dB-35dB signal-to-noise ratio range, the average positioning error of this method is always lower than that of the other four methods. Moreover, it can be seen that this method has stronger anti-interference ability compared with other methods. When it is greater than or equal to 25dB, the positioning error of this method is almost stable within 0.2-0.3m. It can be seen that this method is a positioning technology with high positioning accuracy and strong anti-interference ability.

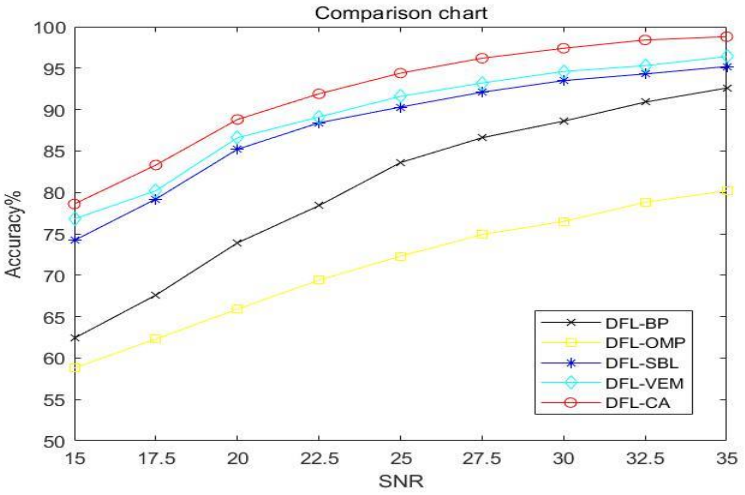

Fig.6: Comparison of positioning accuracy of several positioning algorithms

Figure 6 is a comparison chart of the accuracy of various algorithms under different signal-to-noise ratio conditions. It can be seen more clearly that the proposed method has outstanding advantages in positioning accuracy. After a signal-to-noise ratio greater than 25dB, the positioning is accurate. The performance is as high as 95%, which shows that the positioning accuracy of this method is relatively high.

Based on the analysis of the above results, the multi-target positioning technology fused with the clustering algorithm not only has high positioning accuracy, but also has strong anti-interference ability. In addition, the clustering algorithm is used to achieve the goal of optimizing the target positioning problem without increasing the complexity of the algorithm, and it provides a new idea for the subsequent improvement of positioning accuracy and anti-interference ability.

6. Acknowledgements

Thank you teachers and students for your help. Thank you family and friends for your support and companionship. Thanks to the organizers for the opportunity. Also thank you for your perseverance. Hope to continue to help each other and make progress together in the future study.

7. References

[1] Patwari N , Ash J N , Kyperountas S , et al. Locating the nodes: cooperative localization in wireless sensor networks[J]. IEEE Signal Processing Magazine, 2005, 22(4):54-69.

[2] J. Clerk Maxwell, A Treatise on Electricity and Magnetism, 3rd ed., vol. 2. Oxford: Clarendon, 1892, pp.68–73.

[3] Yassin A, Nasser Y, Awad M. Recent Advances in Indoor Localization: A Survey on Theoretical Approaches and Applications[J]. IEEE Communications Surveys & Tutorials, 2017, 19(99):1327-1346.

[4] D Liu, Sheng B , Hou F , et al. From Wireless Positioning to Mobile Positioning: An Overview of Recent Advances[J]. IEEE Systems Journal, 2014, 8(4):1249-1259.

[5] Wang J, Gao Q, Wang H, et al. Time-of-Flight-Based Radio Tomography for Device Free Localization[J]. IEEE Transactions on Wireless Communications, 2013, 12(5): 2355-2365.

[6] Zan L , Braun T , Dimitrova D C . A time-based passive source localization system for narrow-band signal[C]// 2015 IEEE International Conference on Communications (ICC). IEEE, 2015.

[7] Wang Y , Ho V . An Asymptotically Efficient Estimator in Closed-Form for 3-D AOA Localization Using a Sensor Network[J]. IEEE Transactions on Wireless Communications, 2015, 14(12):6524-6535.

[8] Liu C , Fang D , Yang Z , et al. RSS Distribution-Based Passive Localization and Its Application in Sensor Networks[J]. IEEE Transactions on Wireless Communications, 2016, 15(4):2883-2895.

[9] Liu G , Tang W , Yuzhong L I . Research on Key Technologies of Ultrasonic Phased Array Nondestructive Testing Instrument[J]. Metrology & Measurement Technology, 2018

[10] Feng W , Wang Y W . Indoor Passive Location based on Location Fingerprint[J]. Communications Technology, 2013.

[11] Jiang, Li. Research on Positioning System Based on ZigBee Wireless Sensor Network[J]. Applied Mechanics and Materials, 2014, 687-691:3787-3790.

[12] Shi-Ling M A . Research on signal reconstruction algorithm based on compressed sensing in the ship information center[J]. Ship Science and Technology, 2017.

[13] Xie C J , Lin X U , Zhang T S . Research of image reconstruction of Compressed Sensing using basis pursuit algorithm[J]. Electronic Design Engineering, 2011.

[14] Yang Z Z , YANG. A Survey on Orthogonal Matching Pursuit Type Algorithms for Signal Compression and Reconstruction[J]. Journal of Signal Processing, 2013.

[15] Xu M , Fang Y , Ding W , et al. Topology reconstruction for power line network based on Bayesian compressed sensing[C]// IEEE ISPLC 2015. IEEE, 2015.

[16] Dongping Y U , Xie H E , Yangyang Q I , et al. Variational Bayesian inference based multi-target device-free localization algorithm[J]. Journal of Nanjing University of Posts and Telecommunications(Natural Science Edition), 2018.